Spatial patterns in the tropical forest reveal connections between negative feedback, aggregation and abundance.

Efrat Seri (efrat083@gmail.com)

Nadav Shnerb (nadav.shnerb@gmail.com)

Department of Physics, Bar-Ilan University Ramat-Gan 52900, Israel

Abstract

The spatial arrangement of trees in a tropical forest reflects the interplay between aggregating processes, like dispersal limitation, and negative feedback that induces effective repulsion among individuals. Monitoring the variance-mean ratio for conspecific individuals along length-scales, we show that the effect of negative feedback is dominant at short scales, while aggregation characterizes the large-scale patterns. A comparison of different species indicates, surprisingly, that both aggregation and negative feedback scales are related to the overall abundance of the species. This suggests a bottom-up control mechanism, in which the negative feedback dictates the dispersal kernel and the overall abundance.

Introduction

One of the main characteristics of natural populations, and in particular of sessile species, is their spatial structure. In many cases conspecific individuals are aggregated in space, a phenomena that may be attributed to various mechanisms like dispersal limitation (Borda de Agua et al., 2007; Seri et al., 2012), positive feedback (Kéfi et al., 2007; Scanlon et al., 2007; von Hardenberg et al., 2001) or habitat association. Negative feedback mechanisms, on the other hand, lead to an effective "repulsion" between individuals or clusters (Fort and Inchausti, 2013; Manor and Shnerb, 2008); the excess competition between same-species individuals may induce self-thinning, and the presence of species-specific parasites or predators around an adult tree may decrease the chance of recruitment in its neighborhood.

Turning from populations to communities, the dynamics of ultra-diverse systems like the tropical forest have attracted a lot of interest, as these systems appear to violate a fundamental assumption of natural selection theory, the competitive exclusion principle (Ricklefs and Miller, 2000). Many mechanistic solutions were suggested to this puzzle (Clark et al., 2010; Connell, 1970; Hubbell, 2001; Huisman and Weissing, 1999; Janzen, 1970; McGill, 2003; Tilman, 1994), and almost all of them have to do with some features of these spatial patterns. For example, a competition-colonization tradeoff (Tilman, 1994) implies that the better competitors are more clustered in space. Unfortunately, it is quite difficult to relate directly the spatial patterns to the underlying process, since the details of the dynamics (like the recruitment kernel, or the identity of the best competitor) are usually unknown. Still, by pointing out some generic features of the spatial structure of the forest, an analysis may put severe constraints on the suggested models and may serve as a guide for the establishment and refinement of more realistic hypotheses.

A long-standing hypothesis, aimed to explain the apparent excess biodiversity of the tropical forest, was suggested by Janzen and Connell (Connell, 1970; Janzen, 1970). Basically, the idea is that host-specific enemies (like pathogens or herbivores) are attracted to an adult tree, making its neighborhood hostile to seeds and seedlings of the same species. Accordingly, conspecific individuals effectively repel each other, implying that inferior species may survive in the forest by filling the gaps between superior competitors.

Recently, the Janzen-Connell hypothesis has gained a renewed popularity and attracted a lot of attention, following a few empirical studies that monitor conspecific negative density dependence and tracked its origin. In particular, a substantial decrease of seed efficiency close to a conspecific adult tree was demonstrated (Comita et al., 2010; Swamy et al., 2011), and the reduction in the chance of establishment was attributed to the negative effect of soil biota (Mangan et al., 2010). Moreover, the analysis suggests that the strength of this negative feedback is a good predictor of the commonness/rarity of a species in the tropical forest (Comita et al., 2010; Mangan et al., 2010). Similar results (that locally rare species suffer most from the proximity of relatives) were obtained in subtropical (Liu et al., 2012) and temperate (Johnson et al., 2012) forests.

These new results pose a few interesting questions. The first has to do with the range of the effect. For the Janzen-Connell mechanism to work the negative feedback has to be localized around the adult tree (Nathan and Casagrandi, 2005). How such a localized interaction, with a range of, say, a few meters, can affect the community-wide pattern in tree composition (Hubbell et al., 2001)? What is the mechanism that allows the negative feedback to dictate features of the forest on a much larger scale? One can easily imagine a counter example, where the effect of negative feedback is balanced by another feature. For example, if the seedlings of the "fittest"

species (the one that will select out all other species in the absence of negative-feedback mechanisms) cannot establish at all in a radius of 4 meters around an adult tree, this may be the strongest repulsive effect among all species, still the fittest will be one of the most common species in a 500,000m^2 forest (like the 50-ha plot in Barro-Colorado Island considered below), with more than 10,000 trees, since its offspring win the competition once they are out of the 4m radius.

This brings us to a second question: the relative strength of this negative feedback mechanism, as opposed to well-known processes that lead to aggregation of conspecific individuals, like dispersal limitation (Manor and Shnerb, 2008). While the chance of a seed to germinate, or of a seedling to establish as an adult, may be smaller close to a conspecific tree, the number of attempts (i.e., the number of seed and seedlings in the vicinity of a reproductive individual) is much larger, and the overall pattern will depend on the interplay between these factors. In particular, very strong negative feedback will lead to a lattice-like forest, while strong aggregating forces yield clumped patterns. In fact, it is well known that a pronounced feature of these spatial patterns is aggregation and clustering (Condit et al., 2000; Plotkin et al., 2002; Seri et al., 2012; Zhu et al., 2013), while a direct identification of negative feedback effects from the overall spatial structure of the population has proved itself as quite a difficult task (Zhu et al., 2013). Given that, one may wonder again about the relevance of conspecific local density dependence to the composition of the community.

In this paper we are trying to shed some light on these problems. Analyzing the spatial patterns that emerge from a few generic models and comparing them to the empirical data, we show that local negative effects and "repulsion" between conspecific individuals indeed dominate the

spatial pattern on very short length scales, while aggregation mechanism take over at larger distances.

A more surprising outcome of our analysis emerges when we compare the results for different tree species. It turns out that both the aggregation and the negative feedback are related to the overall abundance of the species in the plot. This phenomenon suggests that the local negative feedback cascades upscales (perhaps by controlling the typical recruitment length) to yield the global pattern. While we cannot suggest a specific mechanistic explanation for these features, we can extract some severe constraints on the possible models of forest dynamics.

This paper is organized as follows. In the methods section we explain the usage of variance-mean ratio and present the results of our analysis for point patterns obtained from a few well-known mechanistic models. The results section is devoted to the analysis of empirical data from the Barro-Colorado island plot (BCI) (Condit and R, 1998; Hubbell and Foster, 1983; Hubbell et al., 2005; Hubbell et al., 1999), in comparison with the patterns surveyed in the methods, emphasizing the universality of the empirical patterns. Finally, we discuss our result in the general context of variance-mean ratio (Taylor's law) and analyze the apparent insights.

Methods

The method we implement in this paper is a multiscale analysis of the variance-mean ratio (VMR, also known as index of dispersion, Fano factor). As we shall see, the VMR technique allows for a direct demonstration of both negative feedback and aggregation on different scales.

An analysis of the spatial deployment of a single population, or a comparison between two or many populations in a community, may be done using either objective scales (like meters) or by using a species specific length scale, like the average distance between neighboring trees. In a recent work (Seri et al., 2014), we have suggested that the second method (intrinsic scales) provides a better insight, at least for the tropical forest we have examined. Using other methods of point pattern distribution analysis (nearest neighbor distance distribution, correlation length and cluster statistics), we discovered that spatial patterns of different species obey a universal scaling law once the length is normalized by the typical distance between conspecific trees $\ell_{0i} = \sqrt{A/N_i}$, where A is the area of the plot and N_i is the abundance of the i-th species in the area A. Following these results we implemented here two versions of the VMR analysis: one is based on objective scales, the other utilizes the species specific scale ℓ_{0i}. As seen in the results section, the VMR analysis seems to support the conclusions of (Seri et al., 2014), suggesting that spatial patterns of different species are becoming similar once the distances are normalized (for every species) by ℓ_{0i}.

The index of dispersion is defined, in general, as the ratio between the variance and the mean of a random variable. Here we are looking at a population, i.e., all the individuals of the focal species *i* in the BCI 50-hactar plot. We start by covering the plot area by a rectangular mesh of

lattice constant ℓ (so that the area of each cell is $\ell \times \ell$), and counting the number of individuals in any box. The mean number of individuals of the *i*-th species in one of those grid cells will be $N_i \ell^2 / A$ and the variance (calculated between the number of individuals in all grid cells) depends on the spatial arrangement of the population. The variance mean ratio (VMR) will be a small number if each box contains, more or less, the same number of individuals and will be large when some boxes are almost empty and others are densely occupied so the population is clustered. The degree of clustering may depend on the length scale; accordingly, by plotting the VMR over scales one obtains a summary of the aggregation properties of the system.

Throughout this paper we present two types of plots. One is a plot of VMR versus the box area $s = \ell^2$, the other is a plot of VMR versus the normalized area $\tilde{s} = \left(\ell / \ell_{0i}\right)^2$. In the last case length is measured in units of ℓ_{0i} and $\tilde{s}$ indicates the mean number of focal species trees in a box.

To wit, let us start with some examples of the VMR-s plots for a few generic point patterns. The simplest case is the Poisson forest, in which trees are spread randomly all over the area. It is well known that, in such a case, the variance is equal to the mean and the VMR is unity, independent the units length used (Kendal, 2004).

It is interesting to note that the errors introduced by sampling noise also have similar properties. As long as the noise is uncorrelated among boxes, the sampling is equivalent to the multiplication of the population inside each box by a random number taken from some fixed distribution. In such a case the variance is larger than the mean, but the VMR is still independent of scale. These features of the Poisson forest and the sampling noise are demonstrated in Fig. 1.

Now let us consider the opposite case: a lattice forest. In such a forest a single tree occupies the center of each box of side length ℓ_{0i}. All boxes with $\ell > \ell_{0i}$ contain the same number of trees, so the variance and the VMR are both zero. For $\ell < \ell_{0i}$ each box is either empty or filled, (moreover, the mesh does not fit the lattice principle axes, and a very weak spatial disorder becomes relevant) and the VMR is unity. Accordingly, the VMR decreases towards zero as ℓ increases, as illustrated in Fig. 2. This and the next figures were obtained from simulations for BCI like systems, with 50-ha area and abundance scales that resemble those observed in reality. Every line in these figures corresponds to the average of 10 simulations. For the same graphs with error bars, see supplementary data.

In a lattice forest the distinction between objective and abundance-dependent scales is obvious. Since the only length scale in a lattice forest is ℓ_{0i}, a plot of the VMR vs. the dimensionless scale $\tilde{s}$ (for different species with different abundance in the same plot) yields a data collapse. On the other hand, if the VMR is plotted vs. s a different curve is obtained for every species and the lines are ordered: since the decay of the VMR from one (Poisson) to zero (lattice) occurs around $\ell \sim \ell_{0i}$, the curve for the most abundant species is the first to deviate from the Poisson value, then the second and so on.

In general, the decay of the VMR on increasing length scales is a hallmark of negative feedback: when individuals repel each other, either via direct competition or by attracting hostile parasites, the spatial structure becomes lattice-like and the VMR decays at large distances. The opposite happens when individuals are aggregated. Again, at short length scales, the VMR must be Poisson-like, but for larger scales the variance increases faster than the mean, leading to an increasing VMR - s line (Perry and Woiwod, 1992). Figure 3 exemplifies this property for a

fractal forest, a structure suggested as a model for the BCI by Ostling et. al. (2000). In such a fractal forest the typical distance between neighboring conspecific trees is a fixed number $\ell_{fractal}$, but ℓ_{0i} depends on the overall species abundance. As a result, the VMR-s plot (objective scale) shows data collapse for different species, while in the VMR-$\tilde{s}$ the curve deviates from the Poisson value when $\ell_{fractal} \sim \ell$, so the curve of the rarest species starts to increase earlier. These characteristics of the VMR do not depend on any special features of a specific fractal structure (like the random Cantor set used here); they do hold also for other fractals.

A more mechanistic model of spatial aggregation is suggested by models that take into account the details of the underlying birth-death process. In particular, the neutral theory of biodiversity suggests a simple framework, in which at every elementary timestep one tree is chosen to die and is replaced by the offspring of another tree, chosen at random from the neighborhood of the dead individual (Seri et al., 2012). Starting from the founder of the focal species, one can run a simulation of forest dynamics until the desired abundance is reached. This simulation is quite simple, since the assumption of neutrality avoids the need to distinguish between non-focal species. Accordingly, the only parameter that affects the spatial structure is the recruitment kernel, i.e., the chance that an offspring from a tree which is located at a distance r from the dead tree will capture the empty slot.

When the recruitment kernel is infinite (the chance of any tree to replace any other is distance-independent) the forest is Poissonian. Here we consider two generic kernels: the mixed local-global kernel (MLGK) and the Cauchy kernel. Under MLGK, the reproducing tree is chosen, with probability μ, at random from the whole forest and with probability 1-μ from a 2-meter neighborhood of the dead tree (clearly μ=1 is the Poissonian limit). With Cauchy kernel the

chance of an offspring to recruit the empty slot depends on the distance of the mother tree from the dead one and follows the (fat-tailed) Cauchy distribution, $P(r) \sim 1/\left[1+\left(r/\ell_{rec}\right)^2\right]$. In a previous work (Seri et al., 2012) we have tried to fit the cluster statistics of the BCI using these two kernels, and showed that the Cauchy kernel fits much better than the MLGK. Here we apply the VMR analysis to a simulated forest with these kernels, where the parameters used are those that gave the best fit to the BCI in (Seri et al., 2012).

Under neutral dynamics there are two length scales associated with each species: ℓ_{0i} that depends on the abundance and the scale associated with the recruitment kernel, ℓ_{rec}. These scales are independent, and one should expect that the VMR shows substantial deviations from Poisson once $\ell > \ell_{rec}$. Accordingly, Figure 4 shows a clear order (the rare species curves raise first) in the VMR-$\tilde{s}$ plot, while in the VMR-s diagram the data collapse since we have taken the same ℓ_{rec} for all species.

The MLGK kernel yields a spatial structure that resembles the patterns observed for a Cox process (where centers are chosen at random and then trees are spread, again at random, in the neighborhood of each center (Cox, 1955)); dispersal limitations induce clustering only within each local patch, but the large scale structure of the forest is Poissonian. Therefore, the VMR curve in Figure 4 "bends over" towards the Poisson limit for $\ell >> \ell_{rec}$ (since our forest is finite the large ℓ behavior is noisy, but the trend is clear), yielding a hump-shaped graph. For a Cauchy forest (Fig. 5) the length scale associated with the average recruitment radius is infinite and the VMR-area curves are monotonic. In fact, one can fit these curves quite nicely with the expression $a+b\tilde{s}^z$ (Perry and Woiwod, 1992), where for all species $a \approx 1$ (in the short scale

Poissonian regime) and the values of the exponent $z \approx 0.5$ are also abundance independent, reflecting only the features of the recruitment kernel.

The results for all these mechanistic models are summarized in Table 1. Evidently, there are two essential qualitative characteristics for any VMR graph. The first is its behavior along scales, where an increase means aggregation (if VMR is greater than one, this implies that aggregative processes are dominant on that scale) a decrease of the VNR below one implies that negative feedback and repulsion control this scale, and a constant value suggests a Poisson distribution. The second characteristic emerges when the VMR's of species with different abundance is compared. If the typical distance between neighboring trees is ℓ_{0i} the VMR-$\tilde{s}$ diagram shows a data collapse, and the frequent species are the first to leave the Poisson regime in the VMR-s plot. On the other hand, when the typical scale between neighboring trees is independent of ℓ_{0i} (e.g., the recruitment kernel) the collapse is manifested only in the VMR-s plot, and the rare species are the first to show substantial deviations from the Poisson limit in the VMR-$\tilde{s}$ diagram.

Results

Given the insights gained from the analysis of VMR plots for these generic models, we are in position to apply the same method to a real community of trees in the tropical forest. A-priory, one should not expect a perfect data collapse as those observed for the models, since the natural population dynamics is affected by all kinds of stochastic forces, and perhaps the assumption that trees of different species have the same spatial dynamics (e.g., the same recruitment kernel) is, in the best case, only a crude approximation. Still it is interesting to examine the empirical results and to find out if they show any kind of qualitative similarity to the models considered so far.

Figure 6 shows the VMR-$\tilde{s}$ and the VMR-s plots for all the dbh>1cm individuals of the 43 $N_i > 1000$ species in the BCI forest (first census). The gross features of the plot resemble those of the neutral Cauchy forest: a Poisson region for small length scales followed by a power-law growth at large scales (the Fractal forest has also these feature, but the data from the BCI do not show spatial "macro-gaps" like those observed in Fig. 3). In contrast with the results obtained for the MLGK model (Fig. 4) there is no decrease of the VMR curves at large values of s or $\tilde{s}$, meaning that the return to the Poisson limit due to the loss of spatial correlation does not occur, at least at the scale of the plot. This suggests some support to the hypothesis that recruitment kernels are Cauchy or Cauchy-like and agrees (as mentioned above) with our detailed analysis of the spatial patterns for the most abundant species (Seri et al., 2012) and with the fractal analysis of (Borda de Agua et al., 2007). As explained in the discussion section, such a behavior is also compatible with the (spatial version of) Taylor's law.

However, when comparing Fig. 6 with Fig. 5 it is clear that the nice data collapse in the VMR-s plot does not appear in the real data. If any, the VMR-$\tilde{s}$ curves appear to fall in a slightly narrower region and to have a more similar shape. To understand that, we notice that the data collapse in Fig. 5 reflects not only the qualitative characteristics of the recruitment kernel, but also the assumption that all species have the same value of ℓ_{rec}. If all species admit the same functional form (Cauchy) for the kernel, but every species i has its own characteristic length scale ℓ^{i}_{rec}, the VMR curves still look like $a+bs^{z}$ (or $a+b\tilde{s}^{z}$), but the value of b will be species dependent. In Fig. 5, where all species have the same ℓ_{rec}, all the VMR curves start to grow beyond a at this scale and the data (when plotted using non-normalized coordinates) collapse, but this is not the case in nature.

We thus analyze the data further, trying to fit the VMR line of every species with the expression $a+bs^{z}$ as we did in Figure 5(a). For all species our fit yields $a \approx 1$, indicating that the sampling errors are small, as expected for such a comprehensive census. However, as demonstrated in Figure 7, the values of b and z are quite scattered, where b is significantly correlated with the abundance, i.e., that species with large abundance are characterized by larger values of b. For z the results are inconclusive, but the graph suggests that the correlations, if any, are also positive.

Since the level of aggregation is zero (Poisson distribution) when $b=0$ or when $z=0$, and increases when these values increase, Figure 7 seems to indicate that the level of aggregation is positively correlated with the abundance. Taking a second look at a hypothetical fat-tailed recruitment kernel like $P(r) \sim 1/\left[1+\left(r/\ell_{rec}\right)^{\gamma}\right]$ ($\gamma = 2$ is the Cauchy limit) one realizes that the observed value of z is dictated by γ alone (since it reflects the behavior on scales much larger

than ℓ_{rec}) while b is determined mainly by ℓ_{rec}. Accordingly, it appears that abundant species are more aggregated, and that the main mechanism behind this feature is that frequent species have shorter recruitment length, i.e., weaker negative feedback.

This picture may receive some further support from an interesting finding that was discovered when we considered the short-range region of Fig. 6 in more detail. Although the VMR curves at short scales appear to stick to one as expected in the Poisson regime, a zoom into the small *s* region reveals a weak, but pronounced, *repulsion (anti-correlation)* between conspecific trees, with a typical *decline* of VMR below one as observed for a lattice forest (Fig. 8). Although this submetric deep is weak and very noisy, it appears in many species (36 out of the 43 considered here) and, unless it reflects an artifact of the data collection procedure, seems to indicate repulsion. Note that the weakness of the negative feedback signal does not imply that the effect itself is weak, since it competes with the aggregation mechanism (dispersal limitation, say) over all scales.

Amazingly, the negative feedback mechanism demonstrated in fig. 8, seems also to be related to the global scale ℓ_{0i}. First, in the VMR-$\tilde{s}$ plot the lines in the repulsion zone appear to follow a single curve (many lines almost coincide when they decline, although different species leave the "master curve" at different points), while there is no such a feature in the VMR-s. Second, only in VMR-$\tilde{s}$ plot the strength of the repulsion is (negatively) correlated with the height of the VMR in the attractive regime, e.g., at $\ell/\ell_{0i}=1$. This feature is depicted in panels (c) and (d) of Fig. 8, where the attraction at a fixed rescaled distance is plotted against the strength of repulsion (measured by the inverse distance between the minimal value of VMR for a certain

species and the Poisson level at VMR=1). The weaker is the repulsion, the higher is the VMR at $\tilde{s} = \ell / \ell_{0i} = 1$. This correlation does not appear in the VMR-s plot.

A possible (although quite radical) interpretation of our results is that the negative feedback controls both the aggregation and the overall abundance of a species in the forest; hence all these patterns are related to the same scale. It may reflect, for example, an evolutionary development of dispersal strategies which is governed by the negative feedback, so the recruitment kernel increases with the strength of the local negative density dependence, otherwise the loss of seeds in the prohibited zone will lower the species' fitness and will lead to extinction.

Discussion

The scaling of the variance with the mean is known as an interesting statistical parameter used to characterize the fluctuations in a system. In particular, the index of dispersion (ID) is widely used in the analysis of ecological point patterns (Krebs, 1999). The usage of this statistic as an indication for Poisson distribution was criticized by many authors, since the VMR is one for a whole set of non-Poissonian distributions (the so called 'unicornian' distributions (Hurlbert, 1990)) but these distributions, in general, do not keep this unicornian property under spatial rescaling (i.e., they are not "Tweedy" (Kendal, 2004)). The variation of the VMR (Fano factor) over scales is a very common analytic tool in other branches of science and in particular in the analysis of neural spike trains, where the deviations from the Poissonian limit indicate either aggregation or repulsion (Lewis et al., 2001).

One of the popular methods used in ecology to characterize spatial clumpiness is the exponent of the variance-mean curve, or its slope when plotted on a double-logarithmic scale. Comparing the variance-mean relationships of many censuses that involved quadrants of different size, Taylor (Taylor, 1961) decided that the variance scales like a power of the mean, with an exponent $\tilde{b}$ that, in most cases, falls in the region $1 \le \tilde{b} \le 2$. Clearly, the variance-mean slope and the VMR considered here are related and $z = \tilde{b} - 1$. As showed here, Taylor's law cannot hold on small scales (at least for scales that are shorter than the typical distance between two individuals) where the fluctuation statistics must become Poissonian. This observation is compatible with other works that criticized Taylor's conjecture (Perry and Woiwod, 1992).

However, as already suggested by Nedler (Perry and Woiwod, 1992), in the intermediate scales we have found, indeed, a reasonable fit to the variance-mean relation $VMR = a + b\tilde{s}^z$ over 2-3 decades. The exponent *z* appears to be in a narrow range of parameters for almost all the species considered here, with 32 out of 43 species having $0.8 < z < 0.9$. This observation suggests that all species are subject to the same kind of spatial dynamics, where the only difference is the basic length scale associated with the overall abundance of the species in the forest ℓ_{0i}. It also agrees with our new work (Seri et al., 2014), where we show that a few basic characteristics of the spatial structure become similar for all the species under species-specific normalization of the length scale by ℓ_{0i}.

The plots of the VMR along scales, presented here, allow us to suggest a possible underlying mechanism. The weak decrease of the VMR below its Poisson limit is an evidence for a short-range repulsion between conspecific trees. Accordingly, the VMR at any scale reflects the interplay between short-range repulsion and the intermediate range aggregating mechanisms.

As seen from the numerical simulations, when the dynamics has no repulsion the VMR at $\tilde{s}=1$ is decreasing as the abundance is increasing. The fact that this relation is destroyed by the repulsive forces implies that the strength of repulsion is correlated with ℓ_{0i}, i.e., with the overall abundance of the species in the forest. The "universal curve" that characterizes the repulsion in the VMR-$\tilde{s}$ plot (Fig. 8), and the absence of correlations between the repulsion and the VMR at the non-normalized scale $s=10m$, also point toward this hypothesis. It will be interesting to check these results using other point pattern analysis techniques (Diggle, 2003; Perry et al., 2006). If true, these findings appear to be consistent with the conclusion of (Comita et al., 2010; Johnson et al., 2012; Mangan et al., 2010) and others, and to suggest that the repulsive interaction affects the overall abundance since it governs the process that leads to aggregation.

The suggested correlation between negative feedback and abundance seems to put severe restrictions on any proposed underlying mechanistic model. It is clear that in a model where species differ by their competitive ability (i.e., in a site which is far away from any conspecific adult, the seeds/seedlings of species A have a better chance to establish than the seeds/seedlings of species B) this feature will dictate the large-scale abundance and will destroy the correlation between negative feedback and ℓ_{0i}. Accordingly, a minimal model that will preserve the features demonstrated here is a generalized version of Hubbell's neutral model of biodiversity (Hubbell, 2001), in which every species has its own "typical distance" that dictates both the negative feedback and the dispersal kernel, but otherwise all individuals are equal, i.e., the chance of seedlings to capture a site is independent of species identity once all these seedlings are out of the negative feedback zone. Such a model may settle the apparent contradiction between Hubbell's version of the neutral theory, in which species identity has nothing to do with its abundance, and the long distance correlations between the abundance of trees that belong to the

same family pointed out recently by (Ricklefs and Renner, 2012). However, it is not trivial that the nice features of the neutral dynamics, like coexistence and realistic species-abundance distributions in a mainland-island setup, are preserved when a species-specific length scale is introduced. We hope to consider this problem in a future work.

Acknowledgements: We thank David Kessler, Lewi Stone, Joe Wright and Richard Condit for helpful discussions and comments. This work was supported by the Israeli Ministry of Science and Technology TASHTIOT program and by the Israeli Science Foundation grant no. 454/11 and BIKURA grant no. 1026/11. The BCI forest dynamics research project was made possible by National Science Foundation grants to Stephen P. Hubbell: DEB-0640386, DEB-0425651, DEB-0346488, DEB-0129874, DEB-00753102, DEB-9909347, DEB-9615226, DEB-9615226, DEB-9405933, DEB-9221033, DEB-9100058, DEB-8906869, DEB-8605042, DEB-8206992, DEB-7922197, support from the Center for Tropical Forest Science, the Smithsonian Tropical Research Institute, the John D. and Catherine T. MacArthur Foundation, the Mellon Foundation, the Small World Institute Fund, and numerous private individuals, and through the hard work of over 100 people from 10 countries over the past two decades. The plot project is part the Center for Tropical Forest Science, a global network of large-scale demographic tree plots.

Borda de Agua, L., Hubbell, S. P., He, F., 2007. Scaling biodiversity under neutrality. Scaling biodiversity. Cambridge University Press, Cambridge, 347-375.

Clark, J., Bell, D., Chu, C., Courbaud, B., Dietze, M., Hersh, M., HilleRisLambers, J., Ibanez, I., LaDeau, S., McMahon, S., Metcalf, J., Mohan, J., Moran, E., Pangle, L., Pearson, S., Salk, C., Shen, Z., Valle, D., Wyckoff, P., 2010. High-dimensional coexistence based on individual variation: a synthesis of evidence. Ecological Monographs 80, 569-608, doi: 10.1890/09-1541.1.

Comita, L., Muller-Landau, H., Aguilar, S., Hubbell, S., 2010. Asymmetric Density Dependence Shapes Species Abundances in a Tropical Tree Community. Science 329, 330-332, doi: 10.1126/science.1190772.

Condit, R, 1998. Tropical forest census plots. Springer, Berlin.

Condit, R., Ashton, P., Baker, P., Bunyavejchewin, S., Gunatilleke, S., Gunatilleke, N., Hubbell, S., Foster, R., Itoh, A., LaFrankie, J., Lee, H., Losos, E., Manokaran, N., Sukumar, R., Yamakura, T., 2000. Spatial patterns in the distribution of tropical tree species. Science 288, 1414-1418, doi: 10.1126/science.288.5470.1414.

Connell, J. H., 1970. On the role of natural enemies in preventing competitive exclusion in some marine animals and in rain forest trees. In: Gradwell, G. R., Den Boer, P. J., Eds.), Dynamics of Population. Wageningen: Pudoc.

Cox, D. R., 1955. Some Statistical Methods Connected with Series of Events. Journal of the Royal Statistical Society. Series B (Methodological) 17, 129-164.

Diggle, P. J., 2003. Statistical analysis of spatial point patterns.

Fort, H., Inchausti, P., 2013. Tropical Forests Are Non-Equilibrium Ecosystems Governed by Interspecific Competition Based on Universal 1/6 Niche Width. Plos One 8, doi: 10.1371/journal.pone.0082768.

Hubbell, S., Ahumada, J., Condit, R., Foster, R., 2001. Local neighborhood effects on long-term survival of individual trees in a neotropical forest. Ecological Research 16, 859-875, doi: 10.1046/j.1440-1703.2001.00445.x.

Hubbell, S. P., 2001. The unified neutral theory of biodiversity and biogeography. Princeton University Press, Princeton, N.J.

Hubbell, S. P., Foster, R. B., 1983. Diversity of canopy trees in a Neotropical forest and implications for the conservation of tropical trees. In: S. L. Sutton, T. C. W., and A. C. Chadwick, (Ed.), Tropical rain forest: ecology and management. Blackwell, Oxford, pp. 25–41.

Hubbell, S. P., Condit, R., Foster, R. B., 2005. Barro Colorado Forest Census Plot Data.

URL https://ctfs.arnarb.harvard.edu/webatlas/datasets/bci.

Hubbell, S. P., Foster, R. B., O'Brien, S. T., Harms, K. E., Condit, R., Wechsler, B., Wright, S. J., de Lao, S. L., 1999. Light-gap disturbances, recruitment limitation, and tree diversity in a neotropical forest. Science 283, 554-557, doi: DOI 10.1126/science.283.5401.554.

Huisman, J., Weissing, F., 1999. Biodiversity of plankton by species oscillations and chaos. Nature 402, 407-410, doi: 10.1038/46540.

Hurlbert, S. H., 1990. Spatial-distribution of the montane unicorn. Oikos 58, 257-271, doi: 10.2307/3545216.

Janzen, D., 1970. Herbivores and the number of tree species in tropical forests. American Naturalist 104, 501-+, doi: 10.1086/282687.

Johnson, D., Beaulieu, W., Bever, J., Clay, K., 2012. Conspecific Negative Density Dependence and Forest Diversity. Science 336, 904-907, doi: 10.1126/science.1220269.

Kendal, W. S., 2004. Taylor's ecological power law as a consequence of scale invariant exponential dispersion models. Ecological Complexity 1, 193-209, doi: 10.1016/j.ecocom.2004.05.001.

Krebs, C. J., 1999. *Ecological Methodology*. Addison-Wesley Longman, Menlo Park, California

Kéfi, S., Rietkerk, M., Alados, C. L., Pueyo, Y., Papanastasis, V. P., Elaich, A., de Ruiter, P. C., 2007. Spatial vegetation patterns and imminent desertification in Mediterranean arid ecosystems. Nature 449, 213-7, doi: nature06111 [pii] 10.1038/nature06111.

Lewis, C. D., Gebber, G. L., Larsen, P. D., Barman, S. M., 2001. Long-term correlations in the spike trains of medullary sympathetic neurons. Journal of Neurophysiology 85, 1614-1622.

Liu, Y., Yu, S., Xie, Z., Staehelin, C., 2012. Analysis of a negative plant-soil feedback in a subtropical monsoon forest. Journal of Ecology 100, 1019-1028, doi: 10.1111/j.1365-2745.2012.01953.x.

Mangan, S., Schnitzer, S., Herre, E., Mack, K., Valencia, M., Sanchez, E., Bever, J., 2010. Negative plant-soil feedback predicts tree-species relative abundance in a tropical forest. Nature 466, 752-U10, doi: 10.1038/nature09273.

Manor, A., Shnerb, N. M., 2008. Facilitation, competition, and vegetation patchiness: from scale free distribution to patterns. J Theor Biol 253, 838-42, doi: S0022-5193(08)00191-4 [pii] 10.1016/j.jtbi.2008.04.012.

McGill, B. J., 2003. A test of the unified neutral theory of biodiversity. Nature 422, 881-5, doi: nature01583 [pii]

10.1038/nature01583.

Nathan, R., Casagrandi, R., 2005. A simple mechanistic model of seed dispersal, predation and plant establishment: Janzen-Connell and beyond.(vol 92, pg 733, 2004). Journal of Ecology 93, 852-852.

Ostling, A., Harte, J., Green, J., 2000. Self-similarity and clustering in the spatial distribution of species. Science 290, 671.

Perry, G. L., Miller, B. P., Enright, N. J., 2006. A comparison of methods for the statistical analysis of spatial point patterns in plant ecology. Plant ecology 187, 59-82.

Perry, J. N., Woiwod, I. P., 1992. Fitting taylor power law. Oikos 65, 538-542, doi: 10.2307/3545573.

Plotkin, J., Chave, J., Ashton, P., 2002. Cluster analysis of spatial patterns in Malaysian tree species. American Naturalist 160, 629-644, doi: 10.1086/342823.

Ricklefs, R., Renner, S., 2012. Global Correlations in Tropical Tree Species Richness and Abundance Reject Neutrality. Science 335, 464-467, doi: 10.1126/science.1215182.

Ricklefs, R. E., Miller, G. L., 2000. Ecology. W.H. Freeman, New York.

Scanlon, T. M., Caylor, K. K., Levin, S. A., Rodriguez-Iturbe, I., 2007. Positive feedbacks promote power-law clustering of Kalahari vegetation. Nature 449, 209-12, doi: nature06060 [pii] 10.1038/nature06060.

Seri, E., Maruvka, Y. E., Shnerb, N. M., 2012. Neutral Dynamics and Cluster Statistics in a Tropical Forest. American Naturalist 180, E161-E173, doi: Doi 10.1086/668125.

Seri, E., Shtilerman, E., Shnerb, N. M., 2014. The glocal forest. Submitted.

Swamy, V., Terborgh, J., Dexter, K. G., Best, B. D., Alvarez, P., Cornejo, F., 2011. Are all seeds equal? Spatially explicit comparisons of seed fall and sapling recruitment in a tropical forest. Ecology Letters 14, 195-201, doi: 10.1111/j.1461-0248.2010.01571.x.

Taylor, L., 1961. Aggregation, variance and the mean. Nature 189, 732-735.

Tilman, D., 1994. Competition and biodiversity in spatially structured habitats. Ecology 75, 2-16.

von Hardenberg, J., Meron, E., Shachak, M., Zarmi, Y., 2001. Diversity of vegetation patterns and desertification. Phys Rev Lett 87, 198101.

Zhu, Y., Getzin, S., Wiegand, T., Ren, H., Ma, K., 2013. The Relative Importance of Janzen-Connell Effects in Influencing the Spatial Patterns at the Gutianshan Subtropical Forest. Plos One 8, doi: 10.1371/journal.pone.0074560.

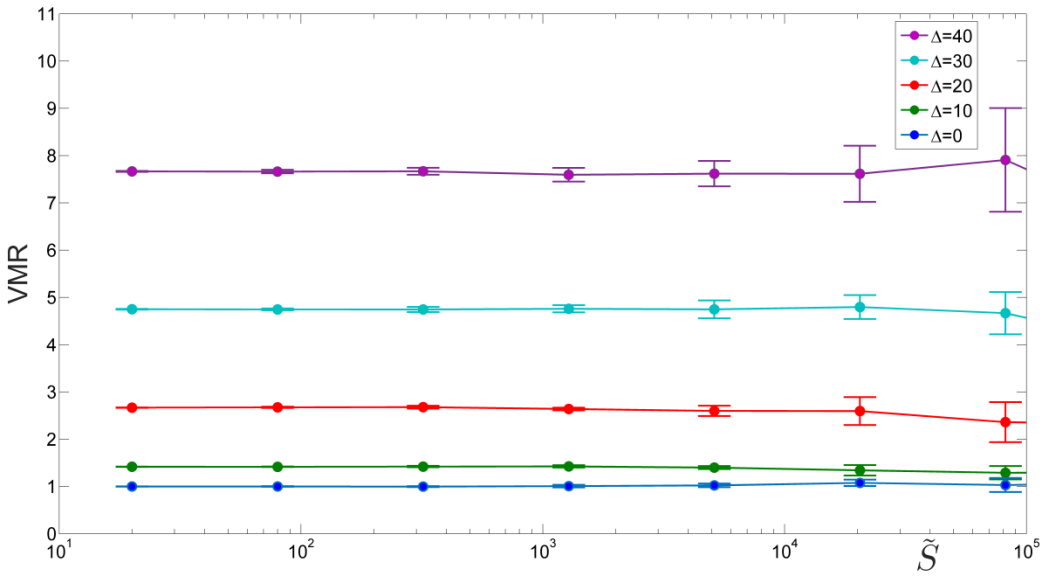

Figure 1. VMR versus $\tilde{s}$ for a Poisson forest, with different levels of sampling error Δ. Error bars show one standard deviation obtained from 10 iterations of the numerical experiment. When there is no sampling error ($\Delta = 0$) the VMR equals unity and is independent of scale as expected. The graphs for $\Delta > 0$ were obtained for different strength of the sampling error. In the simulations, an elementary box of arbitrary area was defined, and for each box j a random number $\eta_j = \Delta \cdot [-0.5, 0.5]$ is assigned. The number of trees at any box was then picked at random from a Poisson distribution with an average $20 + \eta_j$, so for $\Delta = 40$ one obtains the maximal sampling noise. Clearly, sampling errors increase the size of the fluctuations, but (as long as the error is spatially uncorrelated) the VMR curve is still $\tilde{s}$ independent.

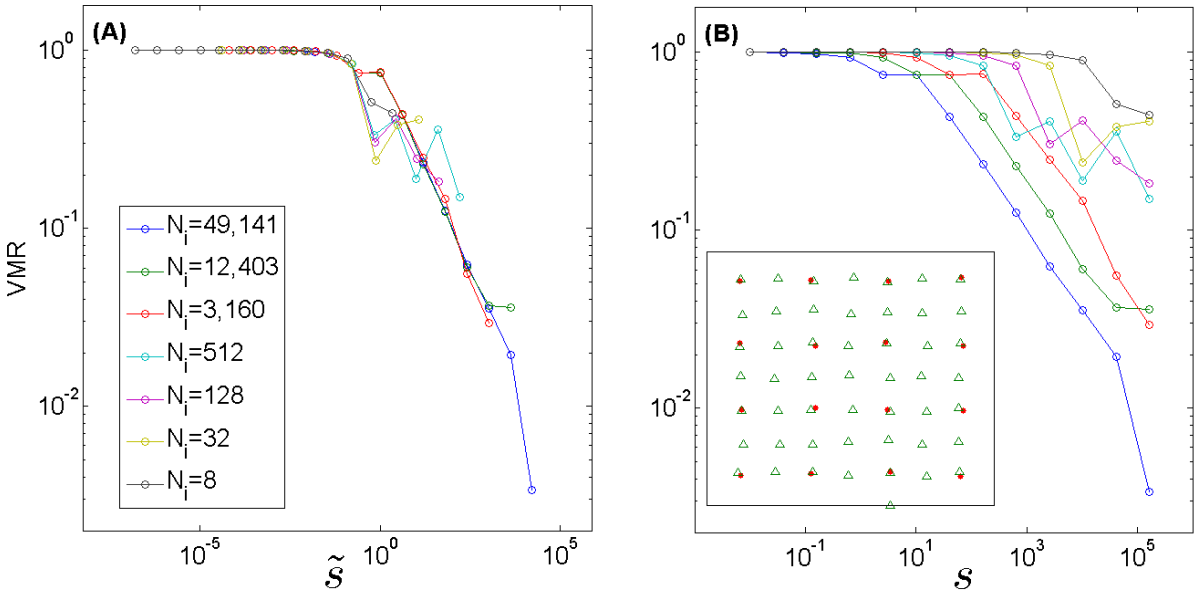

Figure 2. The lattice forest. VMR vs. $\tilde{s}$ (A) and vs. s (B). For every species of N_i trees, a square lattice with unit length ℓ_{0i} admits N_i vertices in a forest of area A. In the simulated forest a single tree is located at random within a fixed distance (much smaller than the lattice constant) around every vertex. Example of a two species (frequent – green triangles, rare – red points) lattice forest is given in the inset of panel (B). The VMR at short length scales is still unity, due to the weak noise, but decreases to zero at large scales, when every box contains the same number of trees. The VMR line shows substantial deviations from the Poisson limit when the average number of trees inside a box is one. Accordingly, the frequent species VMR is the first to decay (panel (B)). On the other hand, when the VMR is plotted against $\tilde{s}$ the curves collapse. The results are shown here for species with different N_i-s, to reflect the range of abundance one finds in the BCI. The mean of 10 curves are presented for every frequency class, where different colors correspond to different N_i-s. The numbers N_i and the size of the plot (a rectangle of 500X1000 meters) were chosen at order to mimic the abundance classes and the area of the BCI forest, both here and in the following figures.

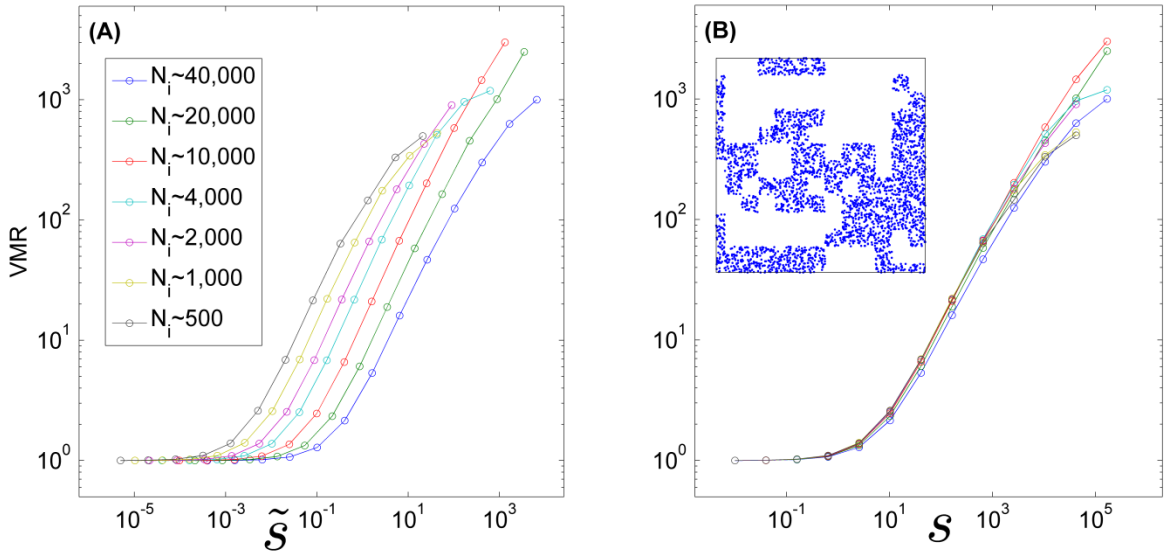

Figure 3. The fractal forest: VMR for a random Cantor set forest vs. $\tilde{s}$ (A) and vs. s (B). We have run the algorithm suggested in Ostling et al., starting with a 2x2 array. Each cell is chosen to be empty with probability P or to be "active" with probability 1-P. An active cell is then divided into 4 equal squares and the process is iterated. The process (using P=0.75) stopped when the forest reaches a size of 256x256 cells. A single realization of the fractal is shown in the inset of panel (B). The area of any elementary box is defined to be $16m^2$ and n=40 trees were located at random within each active box. Implementing a few realizations of the same algorithm, we were able (due to the randomness of the process) to generate a few sets of focal species trees, sets that have the same fractal structure but different abundance. For the analysis presented below we have grouped together realizations that have, more or less, N_i trees and show the mean of them. As expected, the VMR deviates upward from unity at intermediate length scales. Since the minimal distance between neighboring conspecific trees is independent of the abundance of a species, the curves collapse in the VMR-s plot, while in the VMR-$\tilde{s}$ plot the rarer is the species, the lower is the point in which its curve begins to bend upward.

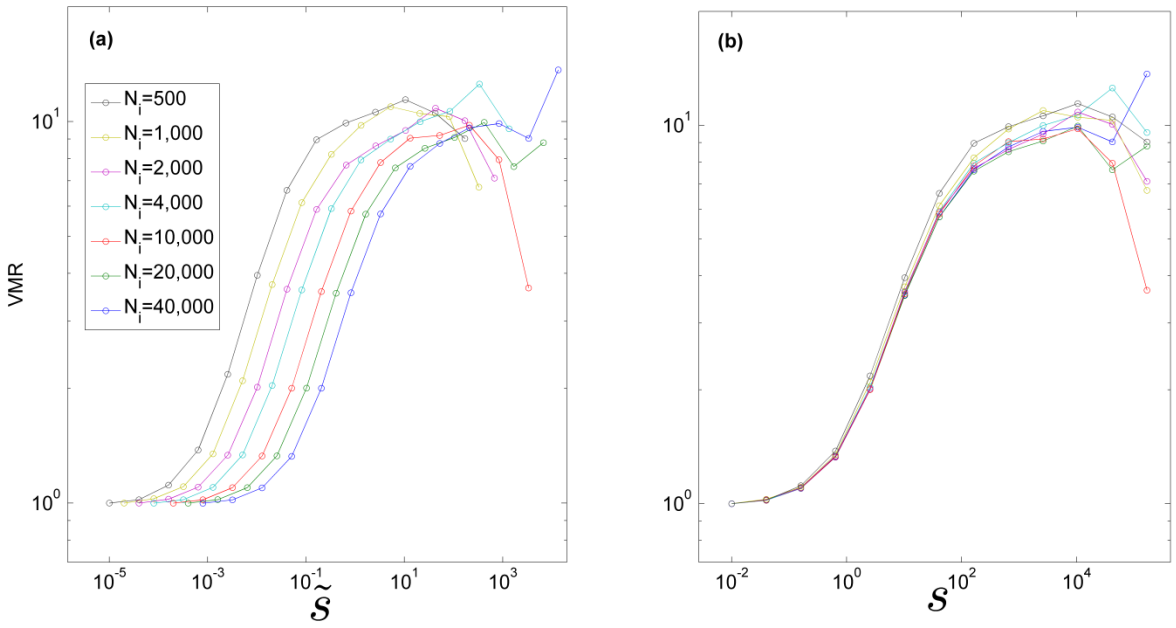

Figure 4. A neutral forest with local-global recruitment kernel. VMR vs. $\tilde{s}$ (A) and vs. s (B). The dynamics is neutral, and the LG recruitment kernel is applied with $\mu = 0.1$, which is the best fit parameter to the cluster size statistics (Seri et al., 2012). To imitate the BCI forest the simulations run over 500x1000 m rectangle, with a neutral dynamics used in (Seri et al., 2012), until the abundance reaches N_i trees. The mean of ten iterations for every value of N_i is shown. The Poisson region is evident on short scales, and clustering manifests itself on the intermediate scales. On larger length scales the curves must return to the Poisson limit, as clusters locations are uncorrelated. Here (for simulations on the scale of the BCI forest, and with the relevant parameters) one can see only the early onset of the decrease. On large scales the curve should return to unity, i.e. to a Poisson forest.

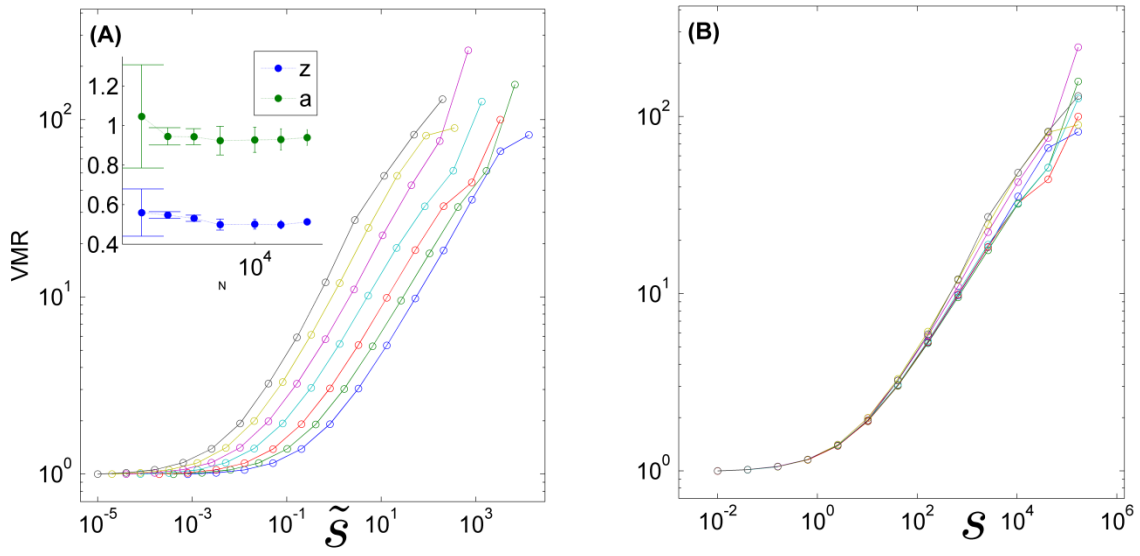

Figure 5. The neutral-Cauchy forest. VMR vs. $\tilde{s}$ (A) and vs. s (B). The dynamic is the same as in fig. 4 but here Cauchy recruitment kernel is applied with $\gamma = 20$, which is the parameter that yields the best fit to the cluster size statistics (Seri et al., 2012). One may see the Poisson region in short scales, and the intermediate scales of clustering, but there is no return to the Poisson limit on large scales. The inset in (A) shows the parameters of the VMR fit to $a + b\tilde{s}^{z}$. The fit for specific species is for the average of 10 iterations and for the 11 first points (the last points are too noisy). R^2 >0.999 for all the fits shown in this figure.

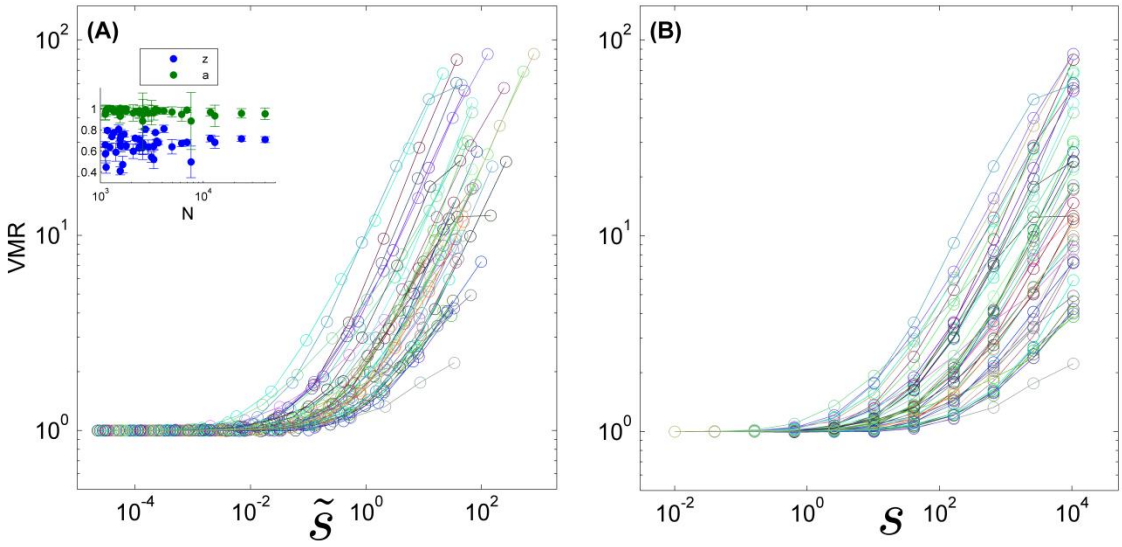

Figure 6. VMR for the real data from the BCI plot. The VMR vs. $\tilde{s}$ (A) and vs. s (B) is shown for all the 43 species with abundance > 1000 trees. The inset in (A) shows the parameters of the fit to $a+b\tilde{s}^{z}$, here in most of the curves R^2>0.99 (except two for which R^2>0.96).

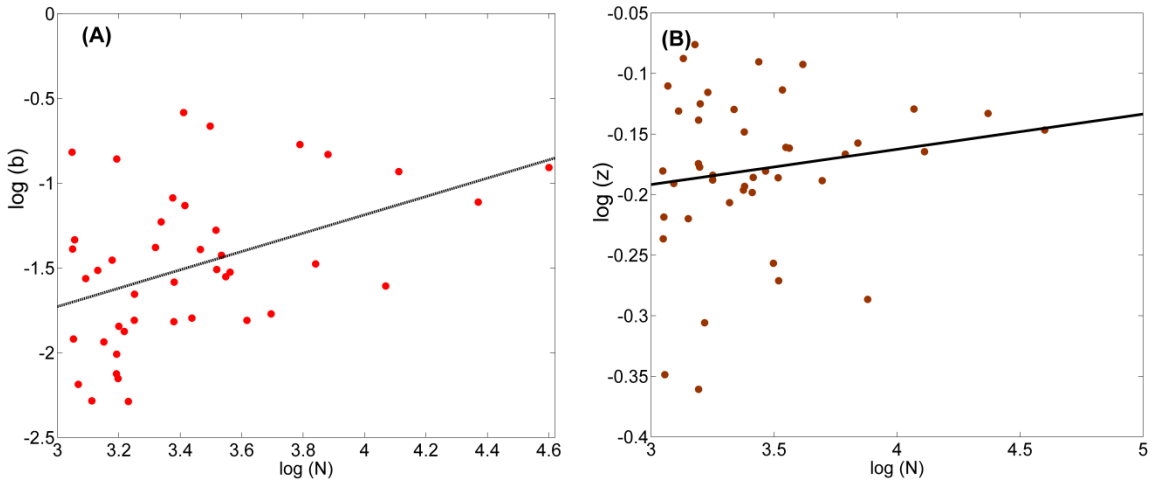

Figure 7: The values of b (panel a) and z (panel b), as extracted by fitting $a+bs^z$ to all the 43 VMR plots of Figure 6, plotted against the abundance N of each species using a double logarithmic scale. The trend line shown at both panel is the result of a linear fit, and seems to indicate a positive correlation between the abundance and the values of b and z. However, only the correlation between N and b is strong and significant (Pearson's $\rho = 0.43$, with P-value 0.004) while the dependence of z on N is, if any, weak and insignificant (Pearson's $\rho = 0.16$, with P-value 0.3).

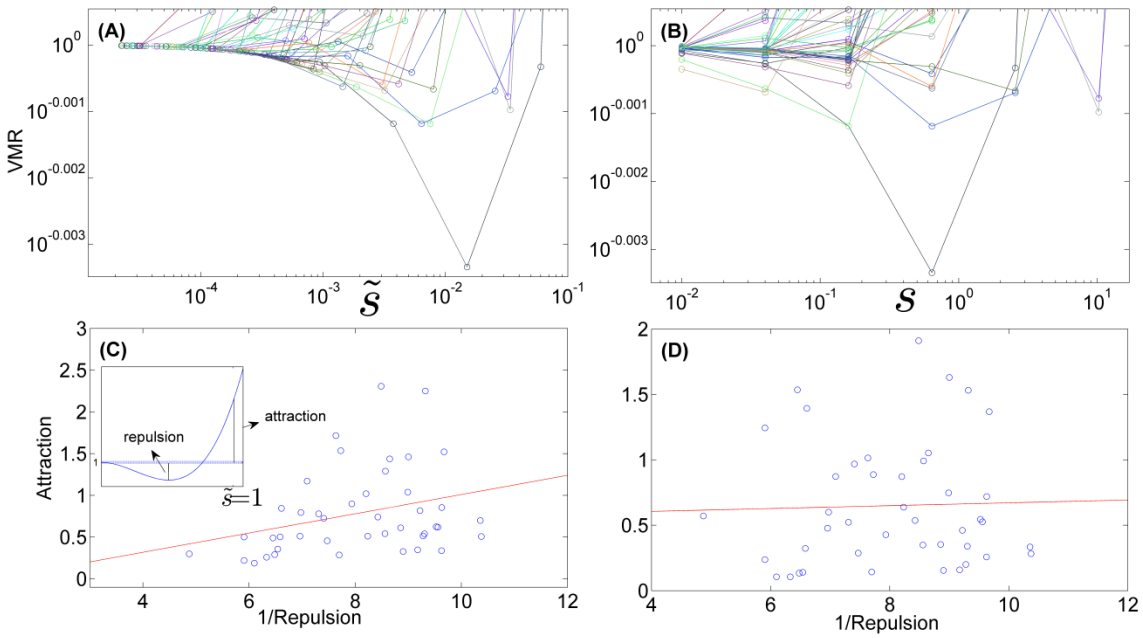

Figure 8. The deep at short length scales. Panels (A-B) show the same datasets presented in fig.6, zooming into the short length scale. In panels (C-D) The attraction parameter (VMR at $\tilde{s}=1$) is plotted against the inverse of the repulsion parameter (VMR at the deep maximum, see the inset of C). The red lines are the linear fit, showing almost no correlation in (D) (Pearson correlation coefficient is 0.03 and the p-value is 0.8) but quite pronounced correlation in (C) (Pearson 0.3, p-value less than 0.05).

Table 1

Length scale that governs the typical distance between neighboring trees	Model(s)	Ecological process	VMR	VMR- s for different N-s	VMR- $\tilde{s}$ for different N-s
ℓ_{0i}	Poisson	Recruitment length scale much larger than any other scale.	Stays fixed	Data Collapse	Data Collapse
ℓ_{0i}	Lattice	Strong negative feedback governs the pattern.	Decreases to zero	No collapse, abundant species are the first to descend.	Data Collapse
Recruitment kernel ℓ_{rec}	MGLK	Neutral dynamics with a mix of local and global recruitment.	Hump-shaped	Data Collapse	No collapse, rare species are the first to ascend.
Recruitment kernel ℓ_{rec}	Cauchy	Neutral dynamics with fat tailed recruitment kernel.	Increases	Data Collapse	No collapse, rare species are the first to ascend.
Fractal unit length	Random Cantor set	Strong environmental filtering.	Increases	Data Collapse	No collapse, rare species are the first to ascend.